

Dirac Electrons on a Sharply Edged Surface of Topological Insulators

Yositake TAKANE and Ken-Ichiro IMURA

*Department of Quantum Matter, Graduate School of Advanced Sciences of Matter,
Hiroshima University, Higashihiroshima, Hiroshima 739-8530, Japan*

(Received

)

An unpaired gapless Dirac electron emergent at the surface of a strong topological insulator (STI) is protected by the bulk-surface correspondence and believed to be immune to backward scattering. It is less obvious, however, and yet to be verified explicitly whether such a gapless Dirac state is smoothly extended over the entire surface when the surface is composed of more than a single facet with different orientations in contact with one another at sharp corner edges (typically forming a steplike structure). In the realistic situation that we consider, the anisotropy of the sample leads to different group velocities in each of such facets. Here, we propose that much insight on this issue can be obtained by studying the electronic states on a hyperbolic surface of an STI. By explicitly constructing the surface effective Hamiltonian, we demonstrate that no backward scattering takes place at a concave 90° step edge. A strong renormalization of the velocity in the close vicinity of the step edge is also suggested.

KEYWORDS: strong topological insulator, Dirac electron, step edge, scattering problem

A single Dirac cone emergent on the surface of a three-dimensional (3D) strong topological insulator (STI) is “topologically” protected; its existence guaranteed by the bulk-surface correspondence and by a nontrivial value of the bulk topological invariant of the strong \mathbb{Z}_2 index.^{1,2)} The existence of such a gapless Dirac cone has been repeatedly verified even experimentally by a number of spin-resolved ARPES measurements performed in different realizations of the 3D STI^{3–5)} and is now incontrovertible.⁶⁾ Theorists have also predicted that, unlike weak topological insulators, an STI exhibits a single surface Dirac cone irrespective of the orientation of the surface. However, the ARPES measurements can be carried out only on the perfectly cleaved surface of layered STI samples, i.e., ARPES is restricted to surfaces of some particular easy-to-cleave orientations. It is indeed a much less trivial issue whether the gapless Dirac state observed on such one “good” facet of a crystal is smoothly extended to adjacent ones, eventually covering the entire surface of the sample. Experimentally, such a behavior of the surface Dirac state may be accessible by STM measurements. In ref. 7, an example of such an experiment performed on atomic-scale terraces of an STI has been reported.

The protected gapless surface Dirac state is known to be robust against perturbations that do not break time-reversal symmetry. An electron in a protected surface state exhibits a notable feature, that is, its spin is locked to a particular direction determined by its momentum (spin-to-momentum locking). This implies that the spin direction of an electronic state with wave number \mathbf{k} is orthogonal to that with wave number $-\mathbf{k}$, resulting in the complete suppression of 180° backward scattering. Here we concern ourselves with the transmission through an interface of two Dirac electron systems,⁸⁾ in which the absence of 180° backward scattering naturally plays a central role. Generally, gapless Dirac electrons, such as those found in graphene, are not necessarily immune to

backward scattering at the interface^{9,10)} if the incoming electron is away from the normal incidence. Only an electron normally incident to the interface is forced to be completely transmitted by the absence of 180° backward scattering. The greater the deviation from the normal incidence, the larger the reflection becomes.

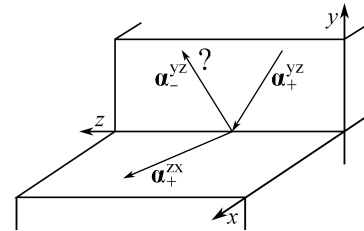


Fig. 1. Concave 90° step edge consisting of two flat surfaces of a 3D STI: one surface is on the yz plane, and the other on the xz plane, and they meet at the z -axis.

Let us focus on the behavior of the protected surface state on the L-shaped wall of an STI (see Fig. 1). This structure can be regarded as a concave 90° step edge consisting of horizontal and vertical facets. Note that both the horizontal terrace and the vertical wall exhibit a protected gapless Dirac cone, since they both separate an STI and a vacuum, two topologically distinct worlds. Although an STI exhibits a protected gapless Dirac cone on surfaces of an arbitrary orientation, it can have, and in practice, it always exhibits anisotropy in its model parameters. As a natural consequence of this, Dirac cones on facets of different orientations (here, those on the vertical and horizontal surfaces) generally have different apertures exhibiting different group velocities. With this taken into account, are these two Dirac cones still smoothly connected without being affected by scattering at the interface, even away from the normal incidence? Naturally, this is an issue closely related to

the corresponding problem in the junction of two pure 2D Dirac systems such as in graphene. In the case of the bulk-surface system we consider, is there any difference in the immunity of the Dirac electrons from scattering processes? These are the issues we would like to address in this letter. We set $\hbar = 1$ below.

To state the problem unambiguously, let us first consider the surface electronic states in the asymptotic regions sufficiently away from the step edge. We focus on a single concave 90° step edge consisting of two semi-infinite surfaces, one on the yz plane and the other on the zx plane (see Fig. 1). The system is assumed to be translationally invariant in the z -direction. By treating each asymptotic region individually, the effective Hamiltonians on the yz and zx planes can be respectively deduced as

$$\mathcal{H}_{\text{eff}}^{yz} = \begin{bmatrix} 0 & -A_y p_y + iB p_z \\ -A_y p_y - iB p_z & 0 \end{bmatrix}, \quad (1)$$

$$\mathcal{H}_{\text{eff}}^{zx} = \begin{bmatrix} 0 & A_x p_x + iB p_z \\ A_x p_x - iB p_z & 0 \end{bmatrix}. \quad (2)$$

We take into account the anisotropy of the (bulk) system, which results in the velocity mismatch, i.e., if $A_x \neq A_y$. We focus on eigenstates with energy $E = [(Ak)^2 + (Bk_z)]^{1/2}$, where $Ak \equiv A_y k_y = A_x k_x$. The corresponding eigenfunctions are

$$\alpha_{\pm}^{yz} = \sqrt{\frac{1}{2A_y}} \begin{bmatrix} 1 \\ \pm e^{\mp i\chi} \end{bmatrix} e^{\mp i k_y y + i k_z z}, \quad (3)$$

$$\alpha_{\pm}^{zx} = \sqrt{\frac{1}{2A_x}} \begin{bmatrix} 1 \\ \pm e^{\mp i\chi} \end{bmatrix} e^{\pm i k_x x + i k_z z}, \quad (4)$$

where $e^{\pm i\chi} = (Ak \pm iBk_z)/E$ and the prefactor is introduced to normalize the probability current in the direction perpendicular to the z -axis. Here, the sign \pm indicates the direction of propagation (see Fig. 1). Let us consider the scattering problem in which α_{+}^{yz} is incident from $y = \infty$. If $k_z = 0$, the reflection into α_{-}^{yz} is forbidden owing to the absence of 180° backward scattering, and hence the incident wave is completely transmitted to α_{+}^{zx} . Here comes the question to be answered:¹¹⁾ does reflection occur when $k_z \neq 0$?

Note that solving a scattering problem at a junction of two inequivalent (velocity-mismatched) Dirac systems is a formidable task. Since one of our primary interests is to examine the continuity of the current density at the corner, we need to deal with a subtle issue related to the discontinuity of the wave functions, which is frequently encountered in the study of Dirac systems.^{8–10)} To overcome such a difficulty, we introduce the following “hyperbolic model” (the details of the model specified later), in which the surface of our 3D STI system with a 90° concave step edge is regarded as a limiting form of a hyperbola (Fig. 2). The two asymptotes of the hyperbolic surface represent the horizontal terrace and the vertical wall meeting at the concave right angle of the STI crystal. Using this hyperbolic model and a set of continuous curvilinear coordinates in terms of this hyperbola, we derive the surface effective Hamiltonian valid over the entire surface, i.e., this provides us with a scheme

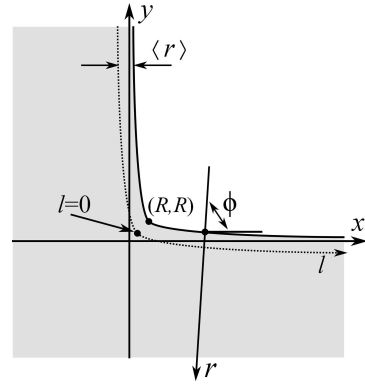


Fig. 2. Cross section (on the xy plane) of our “hyperbolic model”, representing a curved surface of a 3D STI. The cross section of the hyperbolic surface is given by $xy = R^2$, reproducing a 90° step edge in the limit of sufficiently small R .

for treating the two asymptotic surfaces in the framework of a single Hamiltonian.¹³⁾ Note that in the conventional approach, surface electronic states in the two asymptotic regimes, such as those given by eqs. (3) and (4), are derived separately as a solution of two individual uncorrelated problems. Here, we treat them on the same footing to discuss (eventually) how they are connected at the step edge. The treatment of the opposite 90° convex step edge introduces further technical complications in the proposed approach. This last issue will be briefly discussed toward the end of the paper.

Let us start with the following bulk effective Hamiltonian for 3D anisotropic STIs in the continuum limit:^{14, 15)} $H_{\text{bulk}} = m(\mathbf{p})\tau_z + (A_x p_x \sigma_x + A_y p_y \sigma_y + B p_z \sigma_z)\tau_x$, where $p_i = -i\partial_i$ ($i = x, y, z$) and $m(\mathbf{p}) = m_0 + m_2(p_x^2 + p_y^2 + p_z^2)$ is the mass term. Without loss of generality, we assume that $m_0 > 0$ and $m_2 < 0$. The two types of Pauli matrices $\sigma = (\sigma_x, \sigma_y, \sigma_z)$ and $\tau = (\tau_x, \tau_y, \tau_z)$ respectively represent the real and orbital spin degrees of freedom. If the ordinary matrix representation of σ is used, H_{bulk} is expressed as

$$H_{\text{bulk}} = \begin{bmatrix} m(\mathbf{p})\tau_z + B p_z \tau_x & \mathcal{D}_- \tau_x \\ \mathcal{D}_+ \tau_x & m(\mathbf{p})\tau_z - B p_z \tau_x \end{bmatrix}, \quad (5)$$

where $\mathcal{D}_{\pm} = A_x p_x \pm iA_y p_y$. It should be noted that $\mathcal{H}_{\text{eff}}^{yz}$ and $\mathcal{H}_{\text{eff}}^{zx}$ can be derived from H_{bulk} .^{14, 15)}

With the basic assumptions stated, let us introduce an ingenious trick. As mentioned earlier, the main point of our protocol is to consider, instead of directly treating the 90° step edge, the hyperbolic system depicted in Fig. 2. We assume that the intersection of the curved surface with the xy plane is a rectangular hyperbola, $xy = R^2$, and that the 3D STI is translationally invariant in the z -direction. If R is sufficiently small, this surface can be regarded as a concave 90° step edge. It is convenient to introduce curvilinear coordinates, as shown in Fig. 2. Let us draw a straight line that perpendicularly crosses the hyperbola at the crossing point (x_0, y_0) . We define ϕ as the angle between the x -axis and this line, and r as the distance from the crossing point. The Cartesian coordinates (x, y) are expressed as

$$x = -r \cos \phi + x_0(\phi), \quad (6)$$

$$y = -r \sin \phi + y_0(\phi), \quad (7)$$

where $x_0 \equiv R \tan^{\frac{1}{2}} \phi$ and $y_0 \equiv R \cot^{\frac{1}{2}} \phi$. The infinitesimal cross-sectional area is given by $dS = (r + f(\phi))drd\phi$, where

$$f = \sqrt{(\partial_\phi x_0)^2 + (\partial_\phi y_0)^2} = \frac{R}{2 \sin^{\frac{3}{2}} \phi \cos^{\frac{3}{2}} \phi}. \quad (8)$$

The derivatives are expressed as

$$\partial_x = -\cos \phi \partial_r + (r + f)^{-1} \sin \phi \partial_\phi, \quad (9)$$

$$\partial_y = -\sin \phi \partial_r - (r + f)^{-1} \cos \phi \partial_\phi. \quad (10)$$

With these expressions, we can rewrite the mass term as $m(\mathbf{p}) = m_\perp + m_\parallel$ with

$$m_\perp = m_0 - m_2 [\partial_r^2 + (r + f)^{-1} \partial_r], \quad (11)$$

$$m_\parallel = -m_2 [(r + f)^{-2} \partial_\phi^2 - (r + f)^{-3} (\partial_\phi f) \partial_\phi]. \quad (12)$$

Similarly, \mathcal{D}_\pm is rewritten as $\mathcal{D}_\pm = \Omega_\pm + iA_\phi e^{\pm i\tilde{\phi}} \partial_r$, where

$$\Omega_\pm = i(r + f)^{-1} (-A_x \sin \phi \pm iA_y \cos \phi) \partial_\phi, \quad (13)$$

$$e^{\pm i\tilde{\phi}} = (A_x \cos \phi \pm iA_y \sin \phi) / A_\phi \quad (14)$$

with $A_\phi = (A_x^2 \cos^2 \phi + A_y^2 \sin^2 \phi)^{1/2}$.

To derive the surface effective Hamiltonian in the spirit of $k \cdot p$ -approximation, we divide H_{bulk} into two parts as $H_{\text{bulk}} = H_\perp + H_\parallel$, where

$$H_\perp = \begin{bmatrix} m_\perp \tau_z & iA_\phi e^{-i\tilde{\phi}} \partial_r \tau_x \\ iA_\phi e^{i\tilde{\phi}} \partial_r \tau_x & m_\perp \tau_z \end{bmatrix}, \quad (15)$$

$$H_\parallel = \begin{bmatrix} m_\parallel \tau_z + Bp_z \tau_x & \Omega_- \tau_x \\ \Omega_+ \tau_x & m_\parallel \tau_z - Bp_z \tau_x \end{bmatrix}. \quad (16)$$

We first solve the radial eigenvalue equation¹⁴⁻¹⁷ $H_\perp |\psi\rangle = E_\perp |\psi\rangle$ with the boundary condition $|\psi(r=0)\rangle = \mathbf{0}$, that is, all four components of the wave function $|\psi\rangle$ vanish on the surface. As the simplest approximation, we replace $(r + f)^{-1} \partial_r$ in m_\perp with $\langle (r + f)^{-1} \rangle \partial_r$, where the definition of the average $\langle (r + f)^{-1} \rangle$ is given below [see eq. (26)]. Then, we can show that the eigenvalue equation has surface solutions of the damped form, $|\psi\rangle = e^{-\kappa r} |u\rangle$, where κ^{-1} measures the penetration of the surface wave function into the bulk. By superposing two damped solutions,¹⁸ we construct the solution of the radial eigenvalue equation localized near the surface as $|\Psi\rangle = e^{-\kappa_- r} |u_- \rangle - e^{-\kappa_+ r} |u_+ \rangle$. The boundary condition $|\Psi(r=0)\rangle = \mathbf{0}$ holds only when $|u_- \rangle = |u_+ \rangle$ for $\kappa_+ \neq \kappa_-$. As shown in ref. 17, this results in the zero-energy condition $E_\perp = 0$ in our model. We thus find that κ_\pm is given by

$$\kappa_\pm(\phi) = (A_\phi \pm \sqrt{A_\phi^2 + 4m_0 m_2}) / (-2m_2) \quad (17)$$

with $A_\phi \equiv A_\phi - m_2 \langle (r + f)^{-1} \rangle$. We also find that two basis eigenstates, $|+\rangle$ and $|-\rangle$, for H_\perp with zero eigenvalue are given by

$$|\pm\rangle = \frac{1}{\sqrt{c_\phi}} \rho(r, \phi) |\hat{\mathbf{n}} \pm\rangle, \quad (18)$$

where $\rho(r, \phi) = e^{-\kappa_- r} - e^{-\kappa_+ r}$, c_ϕ is a ϕ -dependent nor-

malization constant, and

$$|\hat{\mathbf{n}} \pm\rangle = \frac{1}{2} \begin{bmatrix} e^{-i\tilde{\phi}/2} \begin{pmatrix} 1 \\ \mp i \end{pmatrix} \\ \mp e^{i\tilde{\phi}/2} \begin{pmatrix} 1 \\ \mp i \end{pmatrix} \end{bmatrix}. \quad (19)$$

The real-spin sector $|S_\pm\rangle \equiv (e^{-i\tilde{\phi}/2}, \mp e^{i\tilde{\phi}/2})/\sqrt{2}$ points in the $\pm s_x$ direction in the regime of $y_0 \rightarrow \infty$ ($\phi \rightarrow 0$), while it points in the $\pm s_y$ direction in the regime of $x_0 \rightarrow \infty$ ($\phi \rightarrow \pi/2$). It should be emphasized that when R is very small, $|S_\pm\rangle$ rapidly changes its direction from $\pm s_x$ to $\pm s_y$ across the point $(x_0, y_0) = (R, R)$.

Within the $k \cdot p$ -approximation, any surface state $|\psi\rangle$ can be represented as a linear combination of $|+\rangle$ and $|-\rangle$ with the amplitude respectively specified by α_+ and α_- , i.e., $|\psi\rangle = \alpha_+ |+\rangle + \alpha_- |-\rangle$. The effective surface Hamiltonian $\tilde{\mathcal{H}}_{\text{eff}}$ for the two-component spinor $\tilde{\alpha} = {}^t(\alpha_+, \alpha_-)$ is defined by

$$\tilde{\mathcal{H}}_{\text{eff}} = \begin{bmatrix} \langle + | H_\parallel | + \rangle & \langle + | H_\parallel | - \rangle \\ \langle - | H_\parallel | + \rangle & \langle - | H_\parallel | - \rangle \end{bmatrix}. \quad (20)$$

Here, each matrix element is expressed by

$$\langle \langle \sigma | H_\parallel | \sigma' \rangle \rangle = \int_0^\infty dr (r + f) \frac{\rho(r, \phi)}{\sqrt{c_\phi}} \langle \hat{\mathbf{n}} \sigma | H_\parallel | \hat{\mathbf{n}} \sigma' \rangle \frac{\rho(r, \phi)}{\sqrt{c_\phi}}, \quad (21)$$

where the factor $r + f$ reflects the fact that $dS = (r + f)drd\phi$ and $c_\phi = \int_0^\infty dr (r + f) \rho(r, \phi)^2$. We easily find that $\langle \langle \pm | H_\parallel | \pm \rangle \rangle = 0$. In evaluating the off-diagonal elements, we should note that ∂_ϕ in H_\parallel acts on not only $|\hat{\mathbf{n}} \sigma'\rangle$ but also $\rho(r, \phi)/\sqrt{c_\phi}$. After tedious but straightforward calculations, we find

$$\tilde{\mathcal{H}}_{\text{eff}} = \begin{bmatrix} 0 & \langle + | H_\parallel | - \rangle \\ \langle - | H_\parallel | + \rangle & 0 \end{bmatrix}, \quad (22)$$

where

$$\langle \langle \pm | H_\parallel | \mp \rangle \rangle = -i \frac{\tilde{A}}{\langle r \rangle + f} \partial_\phi - \frac{i}{2} \partial_\phi \left(\frac{\tilde{A}}{\langle r \rangle + f} \right) \pm i B p_z \quad (23)$$

with

$$\tilde{A}(\phi) = [A_\phi - m_2 \langle (r + f)^{-1} \rangle] \partial_\phi \tilde{\phi}. \quad (24)$$

In these equations, we have used the notation

$$\langle r \rangle = \frac{\int_0^\infty dr r \rho(r, \phi)^2}{\int_0^\infty dr \rho(r, \phi)^2}, \quad (25)$$

$$\langle (r + f)^{-1} \rangle = \frac{\int_0^\infty dr (r + f)^{-1} \rho(r, \phi)^2}{\int_0^\infty dr \rho(r, \phi)^2}. \quad (26)$$

The second term on the right-hand side of eq. (23) is essential in ensuring the hermiticity of $\tilde{\mathcal{H}}_{\text{eff}}$.

It is convenient to introduce the one-dimensional coordinate

$$l = \int_{\pi/4}^\phi d\phi' [\langle r \rangle(\phi') + f(\phi')], \quad (27)$$

located slightly beneath the (geometrical) surface (see Fig. 2). Note that the limit of $\phi \rightarrow 0$ ($\pi/2$) corresponds to $l \rightarrow -\infty$ ($+\infty$). We rewrite the effective Hamiltonian

with this coordinate. Since $dl = (\langle r \rangle + f)d\phi$, the wave function $\alpha(l)$ in the new coordinate is related to the old one by $\alpha(l) \equiv \tilde{\alpha}(\phi)/(\langle r \rangle + f)^{1/2}$. From eq. (22), we find that the effective Hamiltonian for $\alpha(l)$ is expressed as

$$\mathcal{H}_{\text{eff}} = \begin{bmatrix} 0 & \tilde{A}p_l + \frac{1}{2}(p_l \tilde{A}) + iBp_z \\ \tilde{A}p_l + \frac{1}{2}(p_l \tilde{A}) - iBp_z & 0 \end{bmatrix} \quad (28)$$

with $p_l \equiv -i\partial_l$. This form of an effective Dirac Hamiltonian has been suggested in ref. 8. The probability current operator in the l direction is given by

$$j_l = \begin{bmatrix} 0 & \tilde{A} \\ \tilde{A} & 0 \end{bmatrix}. \quad (29)$$

Let us consider the behavior of $\tilde{A}(l)$ given in eq. (24), which should be regarded as the effective velocity along the one-dimensional coordinate. Since $f \rightarrow \infty$ in the limit of $l \rightarrow \pm\infty$ [see eq. (8) and the note given below eq. (27)], we observe with the aid of $\partial_\phi \tilde{\phi} = A_x A_y / A_\phi^2$ that $\tilde{A}(-\infty) = A_y$ and $\tilde{A}(\infty) = A_x$. Contrastingly, the velocity can become very large in the close vicinity of the step edge if R is vanishingly small. Note that $m_2 < 0$ is assumed from the outset, and that $f \approx 0$ near $l = 0$ (i.e., $\phi = \pi/4$) if R is very small. The correction term $-m_2(\langle r + f \rangle^{-1})$ in \tilde{A} becomes very large, leading to a large increase in velocity.

Now, we can answer the main question raised earlier. The solution of $\mathcal{H}_{\text{eff}}\alpha = E\alpha$ with $E = [(Ak)^2 + (Bk_z)^2]^{1/2}$ is obtained as

$$\alpha_\pm = \sqrt{\frac{1}{2\tilde{A}(l)}} \begin{bmatrix} 1 \\ \pm e^{\mp i\chi} \end{bmatrix} \exp\left(\pm i \int_0^l dl' \frac{Ak}{\tilde{A}(l')} + ik_z z\right). \quad (30)$$

We see that eq. (30) respectively reproduces eqs. (3) and (4) in the regimes of $l \ll -R$ and $l \gg R$. We also see from eq. (29) that the prefactor $\tilde{A}(l)^{-1/2}$ guarantees current conservation over the entire system. That is, this α_\pm continuously connects the two asymptotic eigenfunctions.¹⁹⁾ In addition, eq. (30) is justified even for vanishingly small (but finite) R . Therefore, we conclude that no reflection takes place at a concave 90° step edge, although the velocity becomes very large in its vicinity and hence the amplitude of the wave function is reduced.

Let us now consider an inverted situation in which the convex side of the hyperbola (see Fig. 2) is filled with a 3D STI. In this situation, our curvilinear coordinates ($r < 0$ and $0 < \phi < \pi/2$) can be applied only to a limited region near the hyperbola of width much smaller than R . Indeed, ∂_x and ∂_y in eqs. (9) and (10) become ill-defined owing to the presence of $(-|r| + f)^{-1}$ if $|r| \gtrsim R$. Therefore, we restrict our analysis on surface states to the case where R is sufficiently larger than the penetration depth $\langle |r| \rangle$. Analysis similar to that reported above reveals that surface states in the convex case are described by an effective Hamiltonian essentially equivalent to eq. (28) but the velocity, now given by $\tilde{A}(\phi) = [A_\phi + m_2(-|r| + f)^{-1}] \partial_\phi \tilde{\phi}$, is reduced [note

the sign change in front of the correction term compared with that in eq. (24)]. This implies that the behavior of surface states in the convex case is essentially equivalent to that in the concave case except that the velocity is renormalized in the opposite way.

We finally comment on the validity of our analysis. Since H_{bulk} is valid in the long-wavelength regime, one may question whether it can be applied to STIs with a sharply edged surface. In eq. (30), the shortest length scale of the derived eigenfunction is on the order of $\langle r \rangle$ even though R becomes vanishingly small. Thus, we expect that our approach will be justified as long as $\langle r \rangle$ is much longer than the lattice constant. This does not necessarily mean that the employed approach allows quantitative predictions of the electronic properties of, for example, atomic-scale terraces of an STI with atomic-scale precision. Yet, our conclusion (no reflection at a single step edge) itself is consistent with the experimental result indicating that topological surface states are transmitted through atomic-scale steps with high probabilities.⁷⁾

Acknowledgment

The authors are supported by KAKENHI: Y.T. by a Grant-in-Aid for Scientific Research (C) (No. 24540375) and K.I. by the “Topological Quantum Phenomena” (No. 23103511).

- 1) L. Fu, C. L. Kane, and E. J. Mele: Phys. Rev. Lett. **98** (2007) 106803.
- 2) J. E. Moore and L. Balents: Phys. Rev. B **75** (2007) 121306.
- 3) D. Hsieh, D. Qian, L. Wray, Y. Xia, Y. S. Hor, R. J. Cava, and M. Z. Hasan: Nature **452** (2008) 970.
- 4) Y. Xia *et al.*: Nat. Phys. **5** (2009) 398.
- 5) Y. L. Chen *et al.*: Science **325** (2009) 178.
- 6) M. Z. Hasan and C. L. Kane: Rev. Mod. Phys. **82** (2010) 3045.
- 7) J. Seo, P. Roushan, H. Beidenkopf, Y. S. Hor, R. J. Cava, and A. Yazdani: Nature **466** (2010) 343.
- 8) R. Takahashi and S. Murakami: Phys. Rev. Lett. **107** (2011) 166805.
- 9) A. Raoux, M. Polini, R. Asgari, A. R. Hamilton, R. Fazio, and A. H. MacDonald: Phys. Rev. B **81** (2010) 073407.
- 10) A. Concha and Z. Tešanović: Phys. Rev. B **82** (2010) 033413.
- 11) The authors of ref. 12 have analyzed this type of problem by requiring the continuity of wave functions at the interface. However, this procedure is questionable since different spin-quantization axes are implicitly used in expressing α_\pm^{yz} and α_\pm^{zx} . Indeed, the spin of α_\pm^{yz} (α_\pm^{zx}) is perpendicular to the s_x -axis (s_y -axis) in the spin space.
- 12) C.-Y. Moon, J. Han, H. Lee, and H. J. Choi: Phys. Rev. B **84** (2011) 195425.
- 13) We consider that the more standard way of connecting the two wave functions (on the opposing sides of a junction) adopted, for example, in ref. 8 is *ad hoc*.
- 14) C.-X. Liu, X.-L. Qi, H. Zhang, X. Dai, Z. Fang, and S.-C. Zhang: Phys. Rev. B **82** (2010) 045122.
- 15) W.-Y. Shan, H.-Z. Lu, and S.-Q. Shen: New J. Phys. **12** (2010) 043048.
- 16) K.-I. Imura, Y. Takane, and A. Tanaka: Phys. Rev. B **84** (2011) 195406.
- 17) K.-I. Imura, Y. Yoshimura, Y. Takane, and T. Fukui: arXiv:1205.4878.
- 18) The radial eigenvalue equation gives four exponentially decreasing (and increasing) solutions. We use the former to construct the two eigenstates of H_\perp compatible with the boundary condition.^{14–17)}
- 19) This result itself is in a sense consistent with the analysis of ref. 12 (see also the comments in ref. 11).